Cold Regions Science and Technology 150 (2018) 35–50

Contents lists available at ScienceDirect

Cold Regions Science and Technology

journal homepage: www.elsevier.com/locate/coldregions

Climate change: Impact on snow loads on structures

Pietro Croce[a], Paolo Formichi[a,*], Filippo Landi[a,b,**], Francesca Marsili[a,c]

[a] Department of Civil and Industrial Engineering-Structural Division, University of Pisa, Largo Lucio Lazzarino, 56126 Pisa, Italy
[b] Institute of Scientific Computing, TU Braunschweig, Mühlenpfordtstrasse 23, D-38106 Braunschweig, Germany
[c] iBMB/MPA, TU Braunschweig, Beethovenstraße 52, 38106 Braunschweig, Germany

ARTICLE INFO

Keywords:
Climate change
Climate models
Extreme values
Snow loads
Snow maps
Monte Carlo simulation

ABSTRACT

A general procedure to evaluate future trends in snow loads on structures is illustrated aiming to study influences of climate change at European scale, to assess its impact on the design of new structures as well as on the reliability levels of existing ones, also in view of definition of updated snow maps for new generation of Eurocodes. Starting from reliable and high quality registered meteorological data of daily temperatures, rain and snow precipitations at nine Italian weather stations, conditional probability functions of occurrence of snow precipitation, accumulation and melting have been preliminarily determined as functions of daily maximum and minimum air temperatures. Based on the above mentioned conditional probability functions, an innovative numerical procedure has been setup, that, starting from daily outputs of climate models in terms of maximum and minimum temperatures and water precipitation, allows, by means of Monte Carlo simulations, to determine the yearly maxima of snow loads for a convenient time interval, 40 years, and then, via the extreme value theory, the characteristic ground snow load. The proposed procedure has been preliminarily validated reproducing data series measured in the above mentioned weather stations in the period 1950–1990 and, subsequently, it has been applied to simulate the evolution of characteristic ground snow loads at these sites in the period 1981–2100. In the analysis, which considered 40 year time windows shifted ten years each time, they have been taken into account not only the forecast data derived by different climate models, but also the reference data, in the period 1981–2005, pertaining to the so-called historical experiments. Finally, the proposed procedure has been implemented in a more general methodology for snow map updating, in such a way that the influence of gridded data, predicted by global climate models, on extreme values of snow loads is duly assessed. Preliminary results demonstrate that the outlined procedure is very promising and allows to estimate the evolution of characteristic ground snow loads and to define updated ground snow load maps for different climate models and scenarios.

1. Introduction

Structural design is often governed by climatic actions, therefore alteration of them caused by climate change could significantly impact the design of new structures as well as the reliability of existing ones. Since in this context, alterations of snow loads are particularly significant, several research groups, based in different areas of the world, are investigating the problem, especially aiming to study the possibility to transfer the outputs of climate models, which refer to geographical cells of large dimensions, on a suitably smaller scale, allowing to derive characteristic values of climatic actions from the above mentioned outputs. More in detail, effects of climate change on snow loads have been recently investigated in Germany (Strasser, 2008), Norway (Tayet et al., 2013) and Canada (CAN/CSA - S502-14, 2014), focusing on their influence on the reliability of the built environment.

In the paper, an innovative and general procedure for the estimation of climate change influence on ground snow loads is presented. Such a procedure, starting from daily outputs of global climate models in terms of maximum and minimum temperatures and water precipitation, allows, by means of Monte Carlo simulations to estimate the yearly maxima of the snow load on the ground and, considering an appropriate time interval, via the extreme value theory, the characteristic snow load on ground. In the proposed procedure, the outputs of global climate models, which are referred to geographical cells with

Abbreviations: CNRM, Centre National de Recherches Météorologiques (Météo France); DMI, Danish Meteorological Institute; E-OBS, European Climate Assessment & Dataset project; ESLRP, European Snow Load Research Project; GCM, General circulation model (global climate model); IPCC, International Panel on Climate change; KNMI, Royal Netherland Meteorological Institute; RCM, Regional climate model; RCP, Representative Concentration Pathway; SWE, Snowfall water equivalent

* Corresponding author.
** Correspondence to: F. Landi, Department of Civil and Industrial Engineering-Structural Division, University of Pisa, Largo Lucio Lazzarino, 56126 Pisa, Italy.
E-mail addresses: p.formichi@ing.unipi.it (P. Formichi), filippo.landi@unifi.it (F. Landi).

http://dx.doi.org/10.1016/j.coldregions.2017.10.009
Received 1 October 2016; Received in revised form 3 June 2017; Accepted 11 October 2017
Available online 14 October 2017
0165-232X/

dimensions of 12.5 up to 25 km, are suitably elaborated, in such a way the snow loads can be defined with a refined geographical resolution, able to take into account also micro-climate effects, depending on the local orography.

The procedure is general enough to permit a sound estimation of future trends in snow loading on structures, aiming more specifically to address the impact of climate change on the assessment of new and existing structures, and can be further enhanced supplementing snow load predictions with data measured in the past, where available, as well as comparing forecasts with experimental measurements.

This research work is motivated in view of the development and the updating of maps of ground snow loads, in the framework of the evolution of the second generation of the structural Eurocodes and, more specifically, of the Eurocode EN 1991 - Part 1–3 - Snow loads (EN 1991-1-3, 2004), as requested in the Mandate M/515 of the European Commission (M/515 EN, 2012) to CEN (European Committee for Standardization) (CEN/TC250, 2013).

2. Snow load on structures: state of art

2.1. Definition of ground snow load

The definition of snow loads on structures in the current version of the structural Eurocodes is largely based upon the results of the European Snow Load Research Project (ESLRP) (DGII-D3, 1998) and, in particular, on the European Ground Snow Load Map, that was one of the most relevant outcomes of that research. This map was the first snow load map derived at European scale with a strong scientific basis (DGII-D3, 1998) and its elaboration started from the analysis of basic snow data collected across 18 European countries, that at that time were members of CEN. By applying extreme value statistics to these observations, the characteristic ground snow loads were derived corresponding to a given probability of exceedance (the 2% upper percentile on yearly basis, corresponding to a return period of approximately 50 years), taking into account both the influence of exceptional snowfalls as well as no snowy winters.

2.2. European snow load maps

Beside the characteristic ground snow loads at weather stations, the above mentioned research (DGII-D3, 1998) allowed to identify ten major European climatic regions, and the corresponding snow maps, elaborated through GIS software. Generally, in each climatic region the ground snow load shows a correlation with the altitude of the site, according to suitably derived laws, except in Norway and Iceland, where snow load is practically independent of the altitude. Based on the above snow map, each National Standard Body of CEN member states, produced its own national map of ground snow load, published in the National Annexes to EN 1991-1-3.

3. Problem statement

3.1. Climate change impacts

The evidence of a warming of the climate system is widely accepted in the scientific community, and since the 1950s, many of the observed changes are unprecedented over decades to centuries (WG1AR5-IPCC, 2013): more precisely, if compared to the pre-industrial level, the increase of the average temperature in the last decade 2001–2011 can be estimated in approximately 0,8 °C at planetary level and around 1.3 °C in Europe (European Environment Agency, 2012).

Consequences of climate change, like alteration of natural processes, modifications of precipitation patterns, melting of glaciers, rise of sea levels and so on, appears increasingly evident. For this reason, whatever the warming scenarios and the level of success of mitigation policies, in the coming decades the impact of climate change needs to be considered, taking into account possible delay in achieving targets in reduction of greenhouse gas emissions as well as adaptation measures to deal with economic, environmental and social consequences of climate change (European Commission, 2013a).

A global assessment of climate change science is presented by the recent IPCC (International Panel on Climate change) Report (WG1AR5-IPCC, 2013). The assessment considers new evidence of past, present and projected future climate change foresees by several independent scientific studies, based on observations of the climate system, theoretical studies of climate processes and simulations using global climate models. Predictions of climate change are usually based on a set of four Representative Concentration Pathways (RCPs) scenarios, that refer to different radiative forcing target levels for the year 2100, in comparison with pre-industrial values (Van Vuuren et al., 2011). Globally, in these scenarios an increase of greenhouse gas emissions generally leads to further warming and changes in the water cycle, but trends, or time variations over time, can be different or even opposite on local scale.

The EU response to climate change is an adaption strategy to enhance the capacity to withstand it and the readiness to respond to its impacts, particularly in most vulnerable key sectors like infrastructures and buildings, characterized by a long life span and high costs (European Commission, 2013a). In this respect, a central role is played by technical standards and by their evolution during the lifetime cycle of the infrastructures and buildings (European Commission, 2013b); implications of climate change for new and existing structures is then a key aspect in the development of second generation of Eurocodes (CEN/TC250, 2013). In this context, the present study aims to determine the effects of Climate Change on snow loads on structures, implementing suitable numerical procedures to derive characteristic snow loads from available data provided by global and regional climate models.

3.2. Snow load in a changing climate

One of the trite remarks about global warming is that, as obvious consequence of it, a reduction of snow is generally expected, but it is not said. In fact, although because of the global warming it is expected that the frequency of snow events should reduce, the intensity of extreme snow events may increase, since the capacity of the atmosphere to hold moisture (and to form snow particles in case of sudden temperature's drop) increases with temperature. This may lead to the increase of both snow density and occurrence of extreme snowfalls in regions where temperatures still may happen to go below freezing level during precipitation events (Strasser, 2008).

The relevance of the problem is confirmed by some spectacular and catastrophic collapses of lightweight roof structures caused by snow, which occurred in the last years all around the Europe (Geis et al., 2012) (Früwald et al., 2007), even if, in some case, snow overloads were accompanied by wrong constructional solutions or insufficient resistance of structural elements (Biegus and Rykaluk, 2009). A wider illustration of some relevant failures can be found in (Geis et al., 2012), while the reliability level of existing structures designed with the current versions of Eurocodes, especially for those structures more sensitive to an increase of snow loads, like lightweight structures of wide-span roofs, is discussed in (Holicky, 2007; Holicky and Sykora, 2009).

To assess the evolution of the ground snow load and its impact on new and existing structures, future trends, in terms of intensity and frequency of precipitations in cold areas, should be compared with those adopted to develop current versions of snow load maps for structural design.

A suitable numerical methodology is proposed to estimate characteristic ground snow loads from available results of global and regional climate models (GCMs and RCMs) in the mid to long term time, according different RCP scenarios. As just said, the interpretation of the outputs of climate models is complicated by their spatial resolution, typically too coarse to study specific sites, which does not allow a direct evaluation of snow load variations over time. For this reason, the

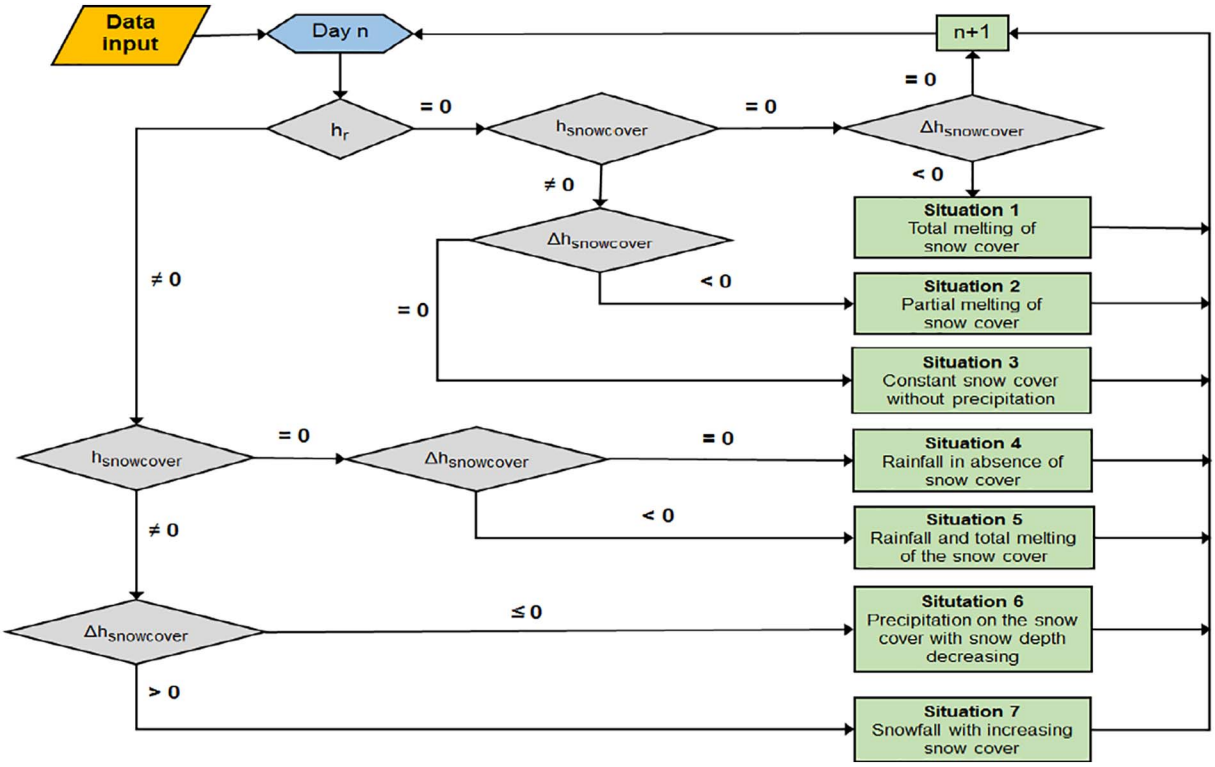

Fig. 1. Flowchart for allocation of daily measured data.

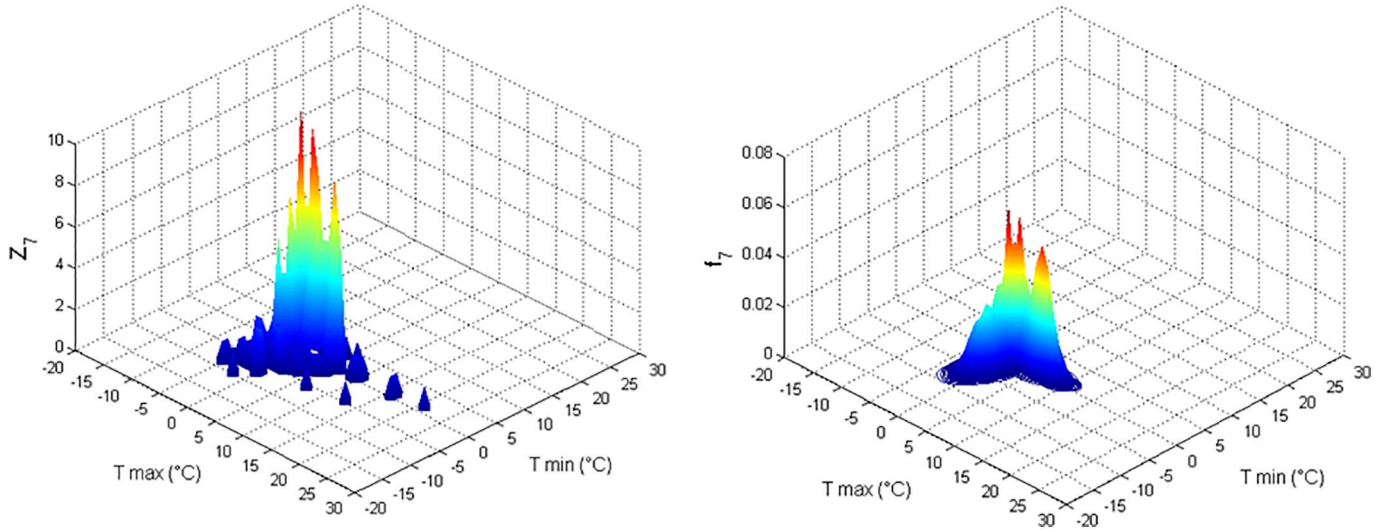

Fig. 2. Frequency histogram for situation 7 (snowfall) Z_7 and consistent probability function f_7 (Bologna-Italy).

proposed procedure has been calibrated and validated against high quality measured data available for time series of 50 or more years and particular attention has been devoted to identify suitable techniques to check the homogeneity of the available data populations.

Finally, it must be stressed that intrinsic uncertainty affecting climate projections in different climate models reflects on their outcomes, so that conclusions about increase/decrease of actions need careful interpretations.

4. Procedure for the estimation of future trends of ground snow loads

The proposed procedure consists of four steps:

- Analysis of observed data series to derive conditional probability functions, linking snowfall and snow melting conditions at a given site with water precipitation data and air temperature;
- Development of a predictive model to evaluate snow loads from available meteorological data;
- Calibration and validation of the model predictions against observed data series;
- Implementation of the model on projected data series provided by global climate change models.

4.1. Analysis of observed data series

Primarily, relevant meteorological data recorded in the past, daily air temperatures and precipitation (water equivalent and snow cover

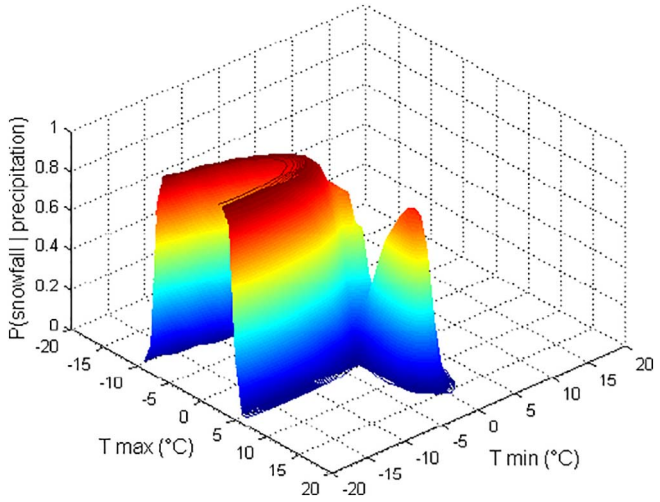

Fig. 3. Conditional probability function of snowfall in presence of precipitation – (Bologna-Italy).

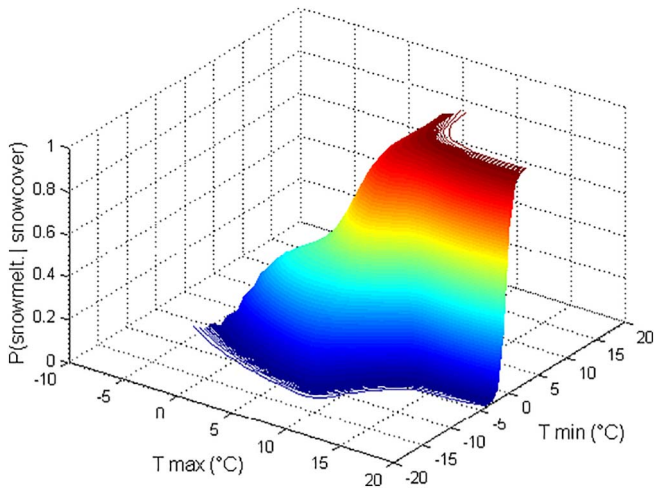

Fig. 4. Conditional probability function of snow melting in presence of snow cover – Italy.

depth), have been collected and analysed. The purpose was to seek the conditions of maximum and minimum daily temperature, T_{max} and T_{min}, at which rainfalls or snowfalls are likely to occur and snow cover depth increases, in case of precipitation of height h_r, or decreases, in case of melting or increasing density of the snow cover.

In particular, seven different situations have been identified comparing day n and day n-1:

1. Total melting of snow cover present at day n-1;
2. Partial melting of the snow cover present at day n-1;
3. Constant snow cover depth without precipitation;
4. Rainfall in absence of snow cover at day n-1;
5. Rainfall and total melting of the snow cover present at day n-1;
6. Precipitation on snow cover with snow depth decreasing;
7. Snowfall with increasing of snow cover;

and, following the flowchart shown in Fig. 1, the daily measured data can be allocated according to them.

Then, for each relevant situation, the frequency histogram $Z(\overline{T}_{min}, \overline{T}_{max})$ has been derived according to the following conditions

$Z(\overline{T}_{min}, \overline{T}_{max})$=number of cases of each situation for which

$$\left(\overline{T}_{max} - \frac{\Delta T}{2}\right) < T_{max,n} < \left(\overline{T}_{max} + \frac{\Delta T}{2}\right) \cup \left(\overline{T}_{min} - \frac{\Delta T}{2}\right) < T_{min,n} < \left(\overline{T}_{min} + \frac{\Delta T}{2}\right)$$

$$-20^{\circ}C < \overline{T}_{min} < 40^{\circ}C; -20^{\circ}C < \overline{T}_{max} < 40^{\circ}C; \Delta T = 1^{\circ}C \quad (1)$$

The seven frequency histograms have been then converted into continuous surfaces $f_j(T_{max}, T_{min})$ by means of up to three two-dimensional Gaussian functions

$$f_j = \sum_i a_i e^{-\frac{1}{2}\left\{\left[\frac{(T_{max}\cos\beta_i + T_{min}\sin\beta_i) - (\mu_{max,i}\cos\beta_i + \mu_{min,i}\sin\beta_i)}{\sigma_{max,i}}\right]^2 + \left[\frac{(T_{min}\cos\beta_i - T_{max}\sin\beta_i) - (\mu_{min,i}\cos\beta_i - \mu_{max,i}\sin\beta_i)}{\sigma_{min,i}}\right]^2\right\}} \quad (2)$$

being i the number of the Gaussian functions, which is assumed equal to the number of modes of the histogram.

In Eq. (2), each Gaussian function is then defined by 6 parameters:

- a_i amplitude
- β_i angle of rotation with respect to x-axis (T_{max})
- $\mu_{max,i}$ median value with respect to x-axis (T_{max})
- $\mu_{min,i}$ median value with respect to y-axis (T_{min})
- $\sigma_{max,i}$ standard deviation with respect to x-axis (T_{max})
- $\sigma_{min,i}$ standard deviation with respect to y-axis (T_{min}).

The parameters β_i, $\mu_{max,i}$, $\mu_{min,i}$ are derived from the peak values of the histograms, while the other parameters, $\sigma_{max,i}, \sigma_{min,i}, a_i$ are estimated by means of least squares method and imposing the condition of unitary volume underlying the surface ($\Sigma_i a_i = 1$).

In Fig. 2 they are shown, as an example, the results obtained in terms of frequency histogram and probability function derived from it, plotted for situation 7 (snowfall) at the Italian weather station of Bologna.

Once derived the probability distribution function f_j for each relevant situation, j = 1, …7, conditional probability functions of snowfall and snow melting for given values of the daily temperatures, $\overline{T}_{max}$ and $\overline{T}_{min}$ are defined. In particular, it results that:

- the conditional probability function of snowfall in presence of precipitation is

$$P(\text{snowfall}(\overline{T}_{max}\,\overline{T}_{min})\text{precipitation}) = \frac{n_7 \cdot f_7}{n_7 \cdot f_7 + n_{4-5} \cdot f_{4-5}} \quad (3)$$

where n_7 is the number of cases of effective snowfall (situation 7) and f_7 is the consistent probability function previously defined; n_{4-5} is the number of cases of rainfall (situations 4 plus 5) and f_{4-5} is the consistent probability function (an example of such a function for the Italian weather station of Bologna is reported in Fig. 3);

- the conditional probability function of melting of snow cover in presence of snow cover is

$$P(\text{snowmelt}(\overline{T}_{max}\,\overline{T}_{min})\text{snowcover}) = \frac{n_{1-2} \cdot f_{1-2}}{n_{1-2} \cdot f_{1-2} + n_3 \cdot f_3} \quad (4)$$

where n_{1-2} is the number of cases of snow melting (situations 1 plus 2) and f_{1-2} is the consistent probability function; n_3 is the number of cases of constant snow cover (situation 3) and f_3 is the consistent probability function previously defined (as example, the conditional probability function obtained considering data of nine Italian weather stations is reported in Fig. 4).

4.2. Predictive model

A predictive model to evaluate ground snow loads has been then

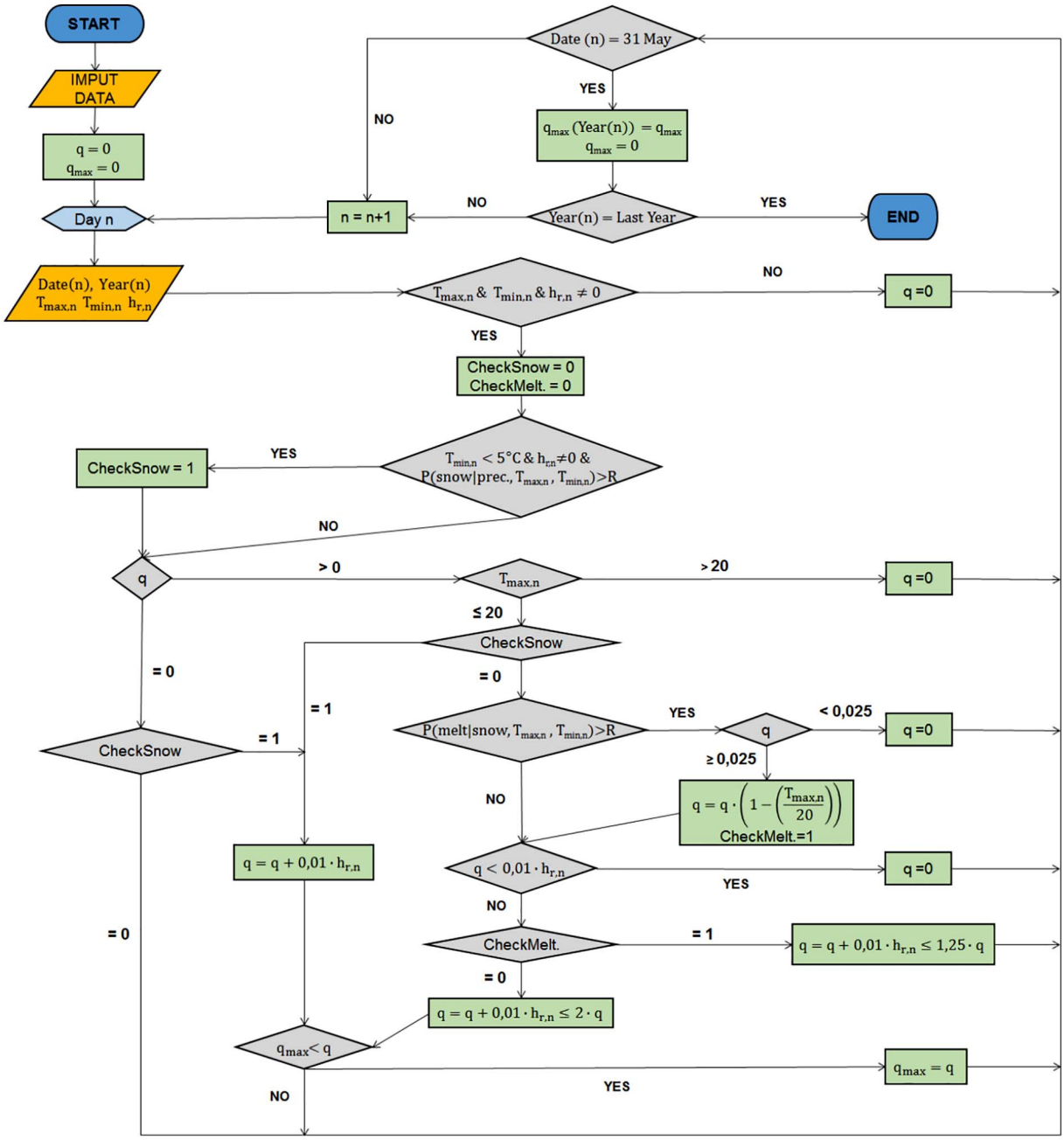

Fig. 5. Flow chart of the algorithm for the estimation of yearly maximum ground snow load.

developed through a suitable Monte Carlo simulation, based on the previously determined conditional *pdfs*.

The flowchart of the implemented algorithm is presented in Fig. 5.

The input data of the algorithm are three relevant meteorological daily data: the maximum and minimum air temperatures, $T_{\max,n}$, $T_{\min,n}$, and the precipitation in mm of water, $h_{r,n}$, at the n-th day.

The probability of snowfall with increasing snow cover depth is estimated by checking the following conditions:

$$T_{\min,n} < 5^{\circ}\mathrm{C} \wedge h_{r,n} \neq 0 \wedge P(\text{snowfall}(T_{\max,n}, T_{\min,n})\text{prec.}) > R \tag{5}$$

where $0 \le R \le 1$ is derived from the randomly generated number, modified with the hypercube Latin sampling technique.

When condition (5) are satisfied, the increase of the ground snow load Δq_n at the n-th day is estimated in terms of water equivalent measured by the rain gauge:

$$\Delta q_n = 0,01 \cdot h_{r,n} \quad \mathrm{kN/m^2} \quad \text{with } h_{r,n} \text{ in [mm]} \tag{6}$$

At the $(n + 1)$-th day, several alternative and mutually exclusive events can happen, with an associated probability of occurrence:

- if snowfall conditions (5) are satisfied again, the ground snow load q_{n+1} is calculated as

$$q_{n+1} = q + 0,01 \cdot h_{r,n+1} \ \mathrm{kN/m^2} \tag{7}$$

- if snow melting conditions are satisfied, i.e.

$$P(\text{snowmelt}(T_{\max,n+1}, T_{\min,n+1})\text{snowcover}) > R \tag{8}$$

snow melts, partially or totally, being R defined before: the melting is assumed to be proportional to the value of $\overline{T}_{max,n+1}$, so that the updated ground snow load becomes

$$q_{n+1} = q_n \cdot \left(1 - \left(\frac{T_{\max,n+1}}{20}\right)\right) \text{ where } 0^{\circ}\mathrm{C} \le \overline{T}_{\max,n+1} \le 20^{\circ}\mathrm{C} \tag{9}$$

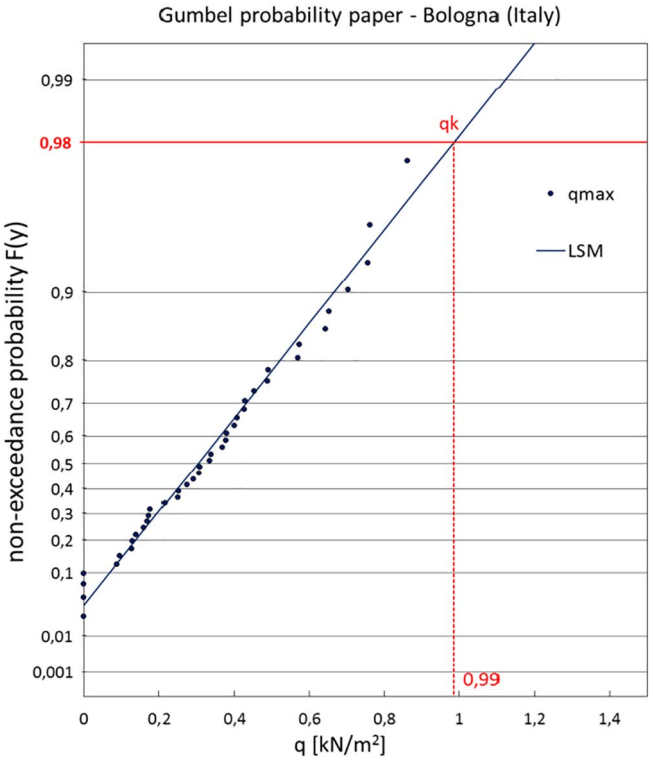

Fig. 6. Estimation of characteristic ground snow load - (Bologna-Italy).

but, if $\overline{T}_{\max,n+1} > 20^{\circ}\mathrm{C}$ or $q_{n+1} < 0,025\frac{\mathrm{kN}}{\mathrm{m}^2}$ total melting is considered.

- if rainfall precipitation occurs in case of snow cover, the new ground snow load is given by

$$q_{n+1} = q_n + h_{r,n+1} \cdot 0,01 \quad \mathrm{kN/m^2} \leq 1,25 \cdot q_n \tag{10}$$

but, if $q_n < 0,01 \cdot h_{r,n+1}$ total melting is considered.

The Monte Carlo simulation considered all days of the year, in order to estimate the yearly maximum ground snow load, $q_{\max}$ and for each year, the process has been iterated 10′000 times. In this way, the Monte Carlo simulation allowed to obtain a series of 10′000 values for maxima $q_{\max}$ for each year and, from them, the expected value of $q_{\max}$, i.e. mean value of the simulated maxima for that year, could been derived. Anyhow, since the results show that mean value and median are very close and that the median value allows to better represent no snowy years, as best estimate of the maximum ground snow load for the examined year the median value $\overline{q}_{\max}$ has been chosen instead of the mean value.

Concerning the number of iterations, calibration exercises to check the convergence of the method, proved that 10^4, 10^5 or 10^6 iterations give practically identical results.

Finally, from the set of the N yearly simulated maxima $\overline{q}_{\max}$, the characteristic value of ground snow load q_k, associated to the probability of 2% to be exceeded in one year (DGII-D3, 1998), has been derived via extreme value analysis. In particular, an extreme value distribution Type I (Gumbel) with parameters μ and σ has been considered, so that the characteristic values have been calculated by

$$q_k = \mu + \sigma \cdot (-\ln(-\ln(1 - 002))) \tag{11}$$

In Fig. 6, as an example, the results are shown for the Italian weather station of Bologna.

4.3. Calibration of the model

The methodology illustrated above has been initially tested against the observed data series of nine Italian weather stations presented in Fig. 7, in which long time series (> 50 years) of high quality daily data of temperatures, precipitation and snow cover height were available.

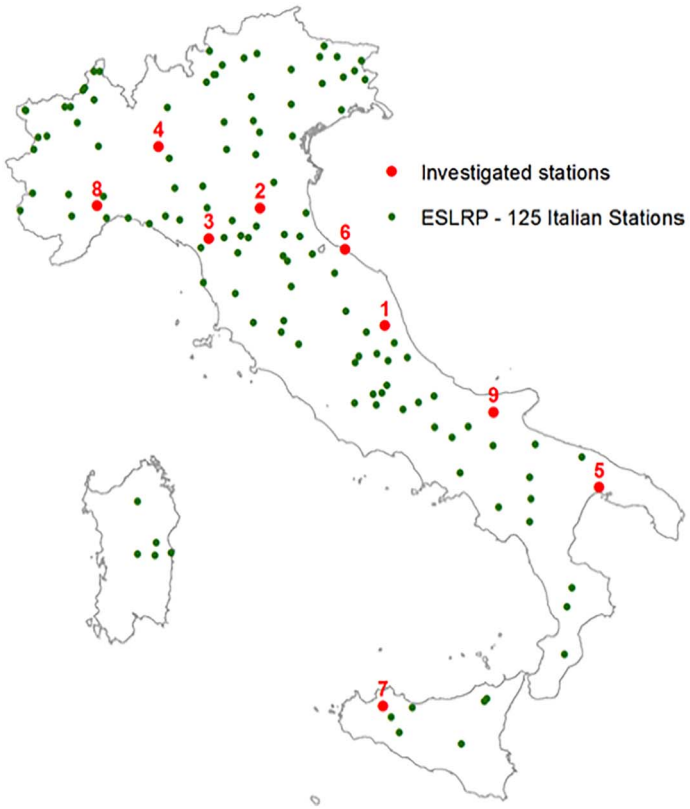

Country	N°	Station	LON [°]	LAT [°]	Altitude [m]	q_{kESLRP} [kN/m²]
IT	1	*Ascoli Piceno*	13,56	42,90	136	1,12
IT	2	*Bologna*	11,36	44,50	51	1,67
IT	3	*Castelnuovo Garfagnana*	10,43	44,12	276	1,14
IT	4	*Lodi*	9,51	45,32	80	1,19
IT	5	*Massafra*	17,13	40,58	116	0,54
IT	6	*Pesaro*	12,91	43,92	11	1,07
IT	7	*San Giuseppe Jato*	13,19	37,97	450	0,94
IT	8	*Spigno Monferrato*	8,36	44,55	476	2,40
IT	9	*San Severo*	15,39	41,68	87	0,74

Fig. 7. Italian weather station used in the analysis.

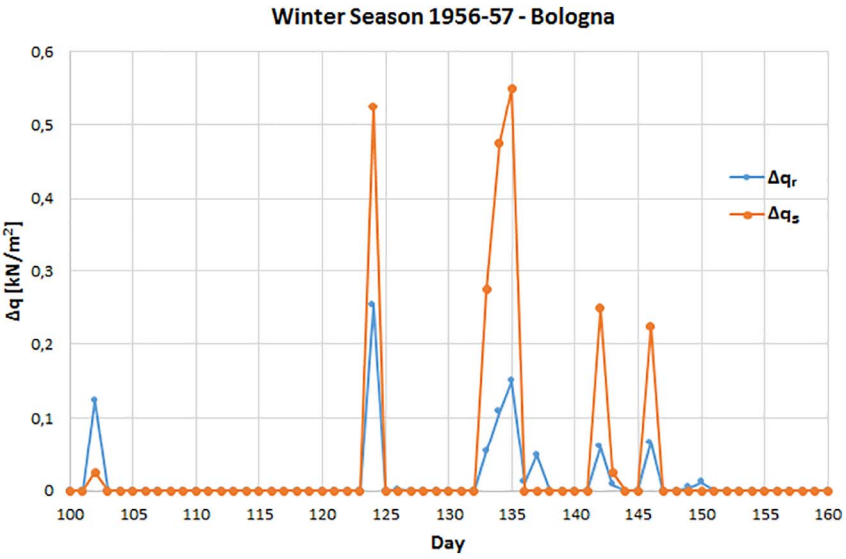

Fig. 8. Comparison of load increase in two consecutive days (Δq_r and Δq_s) for the winter season 1956–57 at Bologna.

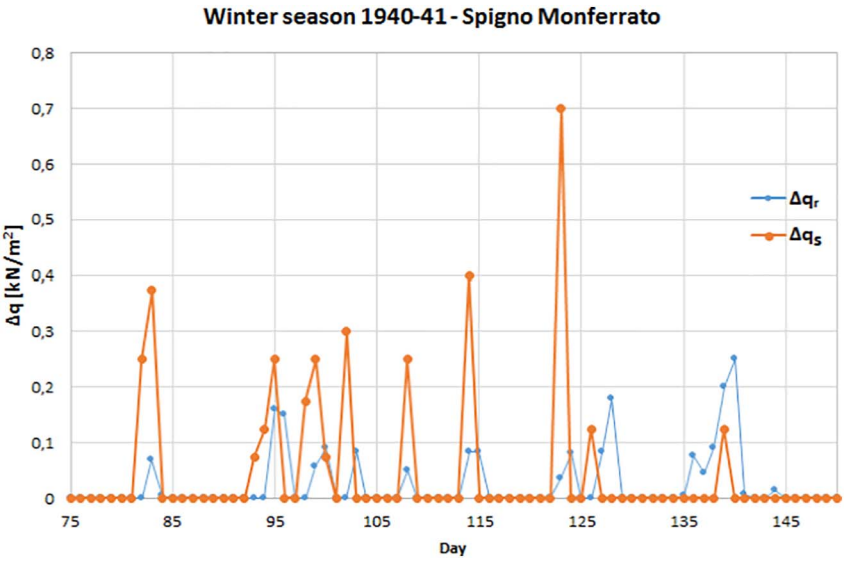

Fig. 9. Comparison of load increase in two consecutive days (Δq_r and Δq_s) for the winter season 1940–41 at Spigno Monferrato.

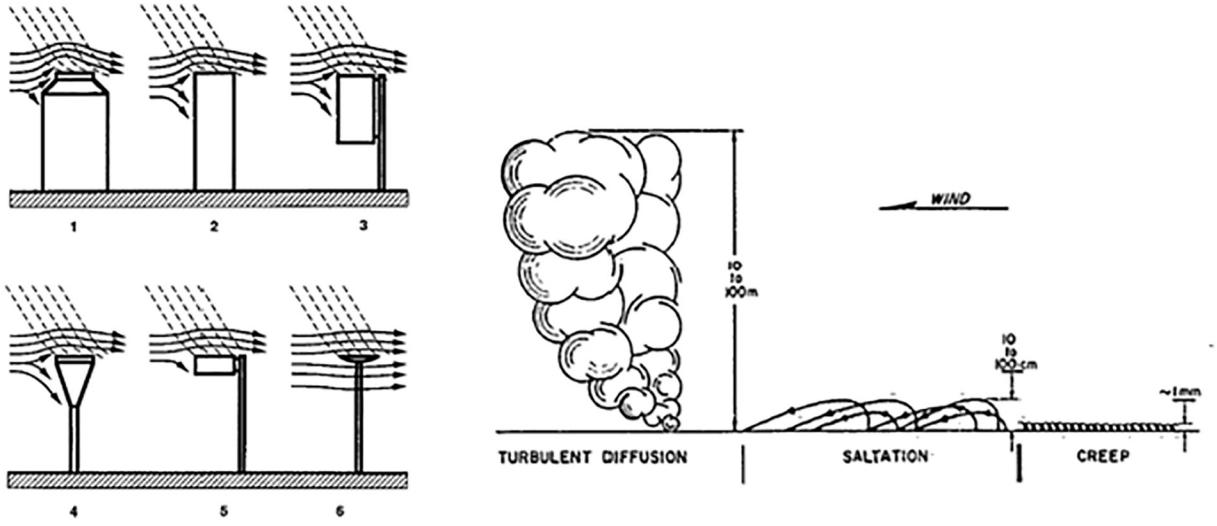

Fig. 10. (a) Wind field deformation at the rain gauge for different shape of precipitation gauges (from (Goodison et al., 1998)) and the three modes of transport for blown snow (from (Mellor, 1965)).

Table 1
Results of the algorithm for ESLRP data.

Country	N°	Weather station	Characteristic ground snow load [kN/m^2]		$K_{corr} = q_k / q_{kESLRP}$
			Tested procedure q_k	ESLRP (DGII-D3, 1998) q_{kESLRP}	
IT	1	*Ascoli Piceno*	0,68	1,12	1,65
IT	2	*Bologna*	0,99	1,67	1,69
IT	3	*Castelnuovo Garfagnana*	1,14	1,14	1,00
IT	4	*Lodi*	0,76	1,19	1,57
IT	5	*Massafra*	0,16	0,54	3,38
IT	6	*Pesaro*	0,67	1,07	1,60
IT	7	*San Giuseppe Jato*	0,50	0,94	1,88
IT	8	*Spigno Monferrato*	0,88	2,40	2,73
IT	9	*San Severo*	0,46	0,74	1,61

These weather stations have been selected among the 125 Italian stations, whose data were collected in the Database of the University of Pisa during the European Snow Load Research Project (ESLRP) (DGII-D3, 1998).

However, in order to compare the results obtained by means of the model on the basis of daily data of temperatures and precipitation at the rain gauges, with those obtained from the ESLRP, combining snow cover depth data with an empirical density law (DGII-D3, 1998), a critical analysis of snow load measurements has to be done.

Indeed, several specific studies have been devoted in the last decades to assess the catching capability of rain, snow or mixed precipitation of different type of rain gauges as well as the influence of wind speed and the efficiency of wind shields (Goodison et al., 1998) (Rasmussen et al., 2012; Yang et al., 1998). A systematic outcome of these studies is that wind speed of 6 m/s at the gauge level (1.5 m above the ground) reduces the snow catching capability of approximately 60% (Yang et al., 1998) or 65% (Rasmussen et al., 2012) in shielded condition, while in unshielded condition the reduction is higher, being around 80%.

For these reasons, snowfall water equivalent (SWE) are often estimated from snow cover depth measurements combined with the estimated snowfall density, according to the formula:

$$SWE = \rho_s \, h_s \ \text{kg/m}^2 \tag{12}$$

where ρ_s is the snow density in kg/m^3 and h_s is the height of snow cover in m. This is what was done for the evaluation of ground snow loads in Italy during the ESLRP (DGII-D3, 1998).

Although snow density can be highly variable, it can be specifically assessed at a given location, so that the application of Eq. (12) leads to acceptable results, even allowing to correct snowfall data recorded by precipitation gauges (Sevruk, 1983; Sevruk, 1986; Lendvai et al., 2014). The Authors indirectly and systematically reached similar findings, comparing the daily increments of the snow loads, obtained in terms of water equivalent from the measurements of the snow height and the corresponding daily solid precipitations measured by the gauges in the considered Italian weather stations.

For the sake of application of Eq. (12), an empirical density law as presented in (DGII-D3, 1998) has been adopted for the snow density, which indicates a reasonable value of $\rho_s = 250$ kg/m^3 for the snow cover density at low altitudes in Italy.

For example, analysing the winter season 1956–57 at the Bologna weather station and the winter season 1940–41 at the Spigno Monferrato weather station, they were obtained the diagrams illustrated in Figs. 8 and 9, respectively. The graphs allow to compare the daily variations of the snow load on the ground, obtained applying Eq. (12) ($\Delta q_s = \Delta h_s \, \rho_s$), represented by the orange lines, with the daily water equivalent of the precipitation measured by the gauge ($\Delta q_r = h_r \, \rho_w$, h_r in m and $\rho_w = 1000$ kg/m^3), represented by the light blue lines.

Examining the diagrams in Figs. 8 and 9, it appears clearly that in Bologna the highest daily rates of snow accumulations are even five times the corresponding accumulation rates derived from the water equivalent of the precipitation measured at the gauge, and that in Spigno Monferrato they reach values up to fourteen. Obviously, as in the calculations it was assumed a snow density of 250 kg/m^3, these huge ratios cannot be justified by a simple overestimation of the actual snow density, because to match the aforementioned values, unrealistic values in the range 20–50 kg/m^3 should be adopted for the snow density.

These systematic errors in solid precipitation measurements at the rain gauges are mainly due to wind field deformation in the neighbourhood of the gauge orifice (Goodison et al., 1998), as summarized in Fig. 10(a) (from (Goodison et al., 1998)); but also snow accumulation due to wind induced transportation phenomena shown in Fig. 10(b) (from (Mellor, 1965)), could increase the snow cover height at the observation site (U.S. Department of Commerce National Oceanic and Atmospheric Administration, 2013), emphasizing the discrepancies between the measured height of the snow cover and that derived on the basis of the water equivalent obtained from gauge measurement.

On the basis of the aforementioned considerations, a suitable correction factor, k, usually $k \geq 1.0$, should be introduced, as proposed in (Sevruk, 1983), to convert water equivalent measurement at the rain gauge into snowfall water equivalent. As recalled, the correction factor

Table 2
Overview on the analysed climate projections and their main characteristics.

Institute	institute_id	RCM name	Resolution	driving_GCM name	driving_ experiment	Period
Danish Meteorological Institute	DMI	HIRHAM5	EUR11 (0.11 deg)	EC-EARTH	historical	1950-2005
	DMI	HIRHAM5	EUR11 (0.11 deg)	EC-EARTH	rcp45	2006-2100
	DMI	HIRHAM5	EUR11 (0.11 deg)	EC-EARTH	rcp85	2006-2100
Météo France	CNRM	ALADIN53	EUR11 (0.11 deg)	CNRM-CM5	historical	1950-2005
	CNRM	ALADIN53	EUR11 (0.11 deg)	CNRM-CM5	rcp45	2006-2100
	CNRM	ALADIN53	EUR11 (0.11 deg)	CNRM-CM5	rcp85	2006-2100
Royal Netherlands Meteorological Institute	KNMI	RACMO22E	EUR11 (0.11 deg)	HadGEM2-ES	historical	1950-2005
	KNMI	RACMO22E	EUR11 (0.11 deg)	HadGEM2-ES	rcp45	2006-2100
	KNMI	RACMO22E	EUR11 (0.11 deg)	HadGEM2-ES	rcp85	2006-2100

Table 3
Characteristic ground snow loads obtained analysing the climate projections.

Cell including the station of	Driving GCM	RCM	Driving Experiment	Period								
				1981-2020	1991-2030	2001-2040	2011-2050	2021-2060	2031-2070	2041-2080	2051-2090	2060-2099
Ascoli Piceno	EC-EARTH	DMI-HIRHAM5	Historical - RCP4.5	3,82	3,78	3,36	2,54	2,33	2,34	2,09	1,74	1,83
			Historical - RCP8.5	3,21	3,25	2,52	1,84	1,94	1,79	2,16	1,35	1,22
	CNRM	CNRM-ALADIN5.3	Historical - RCP4.5	4,71	3,73	3,66	3,35	3,03	3,06	2,54	2,25	2,15
			Historical - RCP8.5	3,78	3,20	2,66	2,48	2,29	2,10	2,02	1,94	1,94
	HadGEM2-ES	KNMI-RACMO22E	Historical - RCP4.5	2,86	2,50	3,06	2,91	2,90	2,86	1,97	1,72	-
			Historical - RCP8.5	2,86	2,54	2,50	2,54	2,50	2,33	1,61	1,40	1,42
Bologna	EC-EARTH	DMI-HIRHAM5	Historical - RCP4.5	1,58	1,63	1,63	1,19	0,55	0,61	0,46	0,57	0,81
			Historical - RCP8.5	1,27	1,30	1,28	1,20	1,30	1,32	1,31	1,14	0,48
	CNRM	ALADIN5.3	Historical - RCP4.5	3,30	3,59	2,63	3,15	2,38	1,84	1,85	1,51	1,46
			Historical - RCP8.5	3,14	2,39	2,20	2,01	2,01	1,92	1,61	1,48	1,46
	HadGEM2-ES	KNMI-RACMO22E	Historical - RCP4.5	1,84	1,78	1,68	1,41	1,36	1,33	1,01	0,94	-
			Historical - RCP8.5	1,61	1,54	1,32	1,21	1,10	1,15	1,05	1,12	0,90
Castelnuovo Garfagnana	EC-EARTH	DMI-HIRHAM5	Historical - RCP4.5	1,19	1,22	1,12	1,06	1,07	1,14	1,11	0,89	1,13
			Historical - RCP8.5	1,25	1,24	1,12	1,03	0,98	0,87	0,76	0,62	0,63
	CNRM	ALADIN5.3	Historical - RCP4.5	7,96	7,41	5,91	5,48	4,58	4,48	3,93	3,86	3,84
			Historical - RCP8.5	7,78	7,51	6,01	5,45	5,23	4,77	4,47	4,03	2,00
	HadGEM2-ES	KNMI-RACMO22E	Historical - RCP4.5	3,58	3,68	3,57	3,00	2,89	2,24	1,95	1,94	-
			Historical - RCP8.5	3,23	3,21	2,31	1,97	1,74	1,65	1,56	1,38	1,33
Lodi	EC-EARTH	DMI-HIRHAM5	Historical - RCP4.5	1,82	2,14	2,07	1,68	1,67	1,01	0,96	0,91	1,12
			Historical - RCP8.5	1,89	2,12	2,01	1,54	1,62	1,39	1,37	1,25	0,78
	CNRM	ALADIN5.3	Historical - RCP4.5	2,20	2,09	1,89	1,72	1,45	1,34	1,31	1,21	1,18
			Historical - RCP8.5	1,96	1,96	1,73	1,52	1,54	1,25	1,21	1,17	0,75
	HadGEM2-ES	KNMI-RACMO22E	Historical - RCP4.5	2,15	2,14	1,95	1,89	1,70	1,52	1,57	1,40	-
			Historical - RCP8.5	2,05	1,97	1,67	1,51	1,33	1,17	1,19	0,94	0,89
Pesaro	EC-EARTH	DMI-HIRHAM5	Historical - RCP4.5	1,17	1,08	0,83	0,92	0,55	0,38	0,72	0,40	0,46
			Historical - RCP8.5	1,02	0,99	0,87	0,80	0,80	0,71	0,54	0,45	0,46
	CNRM	ALADIN5.3	Historical - RCP4.5	0,91	1,05	0,98	0,98	0,93	0,65	0,64	0,41	0,44
			Historical - RCP8.5	0,92	0,86	0,80	0,73	0,64	0,57	0,54	0,42	0,50
	HadGEM2-ES	KNMI-RACMO22E	Historical - RCP4.5	1,25	1,04	1,04	0,51	0,49	0,57	0,53	0,53	-
			Historical - RCP8.5	1,25	1,06	0,94	1,10	1,07	0,64	0,57	0,49	0,25
Spigno Monferrato	EC-EARTH	DMI-HIRHAM5	Historical - RCP4.5	5,25	6,15	5,20	5,36	5,18	5,15	4,79	4,31	4,93
			Historical - RCP8.5	4,42	4,70	4,80	4,64	4,84	4,25	3,75	3,39	3,22
	CNRM	ALADIN5.3	Historical - RCP4.5	7,50	7,37	6,82	6,79	6,59	5,38	5,56	6,54	6,08
			Historical - RCP8.5	7,19	6,80	6,60	6,42	6,42	6,08	5,33	5,25	4,84
	HadGEM2-ES	KNMI-RACMO22E	Historical - RCP4.5	5,61	5,76	5,16	5,41	5,37	5,30	4,65	4,34	-
			Historical - RCP8.5	5,85	5,99	5,41	5,96	5,67	5,57	4,24	3,37	3,37

is mainly depending on the type of the rain gauge employed for the measurements, and on its wind protection, if any; on the location of the weather station, and on the average wind conditions during the precipitation events, so resulting a specific property of the weather station.

As the present study focuses on the extreme values of the snow load, a suitable correction factor, k_{corr}, affecting the characteristic values has been introduced, to convert characteristic snow loads derived from water equivalent measurement at the rain gauges in snow water equivalent (DGII-D3, 1998).

The results of the analysis for the investigated weather stations are reported in terms of characteristic values of ground snow loads (q_k) in Table 1. By comparing these values with those obtained by the ESLRP ($q_{k,\,ESLRP}$), suitable site dependent correction factors, $k_{corr} = \frac{q_k}{q_{k,ESLRP}}$, have been derived, which synthetize all the above mentioned errors affecting the evaluation of the snow water equivalent from solid precipitation measurements at the rain gauge.

Discussion of results in Table 1 clearly demonstrates that k_{corr} can be considered a characteristic parameter of the site and of climatic zone. In effect, it assumes typically values around 1.70, that are comparable with the typical values present in literature (Goodison et al., 1998; Sevruk, 1983; Sevruk, 1986; Lendvai et al., 2014); for instance, in (Sevruk, 1983) conversion factors up to 2.44 are reported for the Alpine region, which are not far from the value determined for Spigno Monferrato, 2.73. Moreover, the high value of the conversion factor in Spigno Monferrato was anticipated by the analysis of the daily increments, as illustrated in the already discussed Fig. 9.

A separate discussion is necessary for the Massafra weather station, characterized by $k_{corr} = 3.38$. In effect, Massafra is an exceptional case, due to the particular site situation, which is in Southernmost part of Italy, in the Taranto Gulf, very close to sea, and it is characterized by a very low number of snowfall events in the investigated period.

4.4. Analysis of climate projections

Once performed the calibration of the procedure against registered data series, which allowed to estimate the correction factor k_{corr}, the analysis has been extended to projected data series provided by different general circulation models (GCMs) and different regional climate models (RCMs) according to different RCPs scenarios (RCP4.5 and RCP8.5) up to the year 2100. In particular, they have been used available high resolution data EUR11 (grid resolution of 12.5 km), developed within the EUROCORDEX initiative (Jacob et al., 2014) (Kotlarsky et al., 2014), for the control period 1981–2005 (*Historical Experiment*), where "run" is forced by observed atmospheric composition changes (Taylor et al., 2012) and for the future period 2006–2100 (*RCPs Experiment*), where "run" is forced by different RCPs scenarios (Taylor et al., 2012).

The characteristics of the investigated climate models and scenarios are summarized in Table 2, and for the following figures the blue colour is assigned to data provided by the Danish Meteorological Institute (DMI), the green colour to data provided by CNRM (Centre National de Recherches Météorologiques de Météo France) and orange colour to the Royal Netherland Meteorological Institute (KNMI).

The analysis has been carried out for subsequent time windows, each spanning over forty years; the obtained estimates of characteristic ground snow loads (q_k) are presented in Table 3 and their variations over time are illustrated in Fig. 11 for some of the nine tested Italian weather stations, considering different "40 years" time windows,

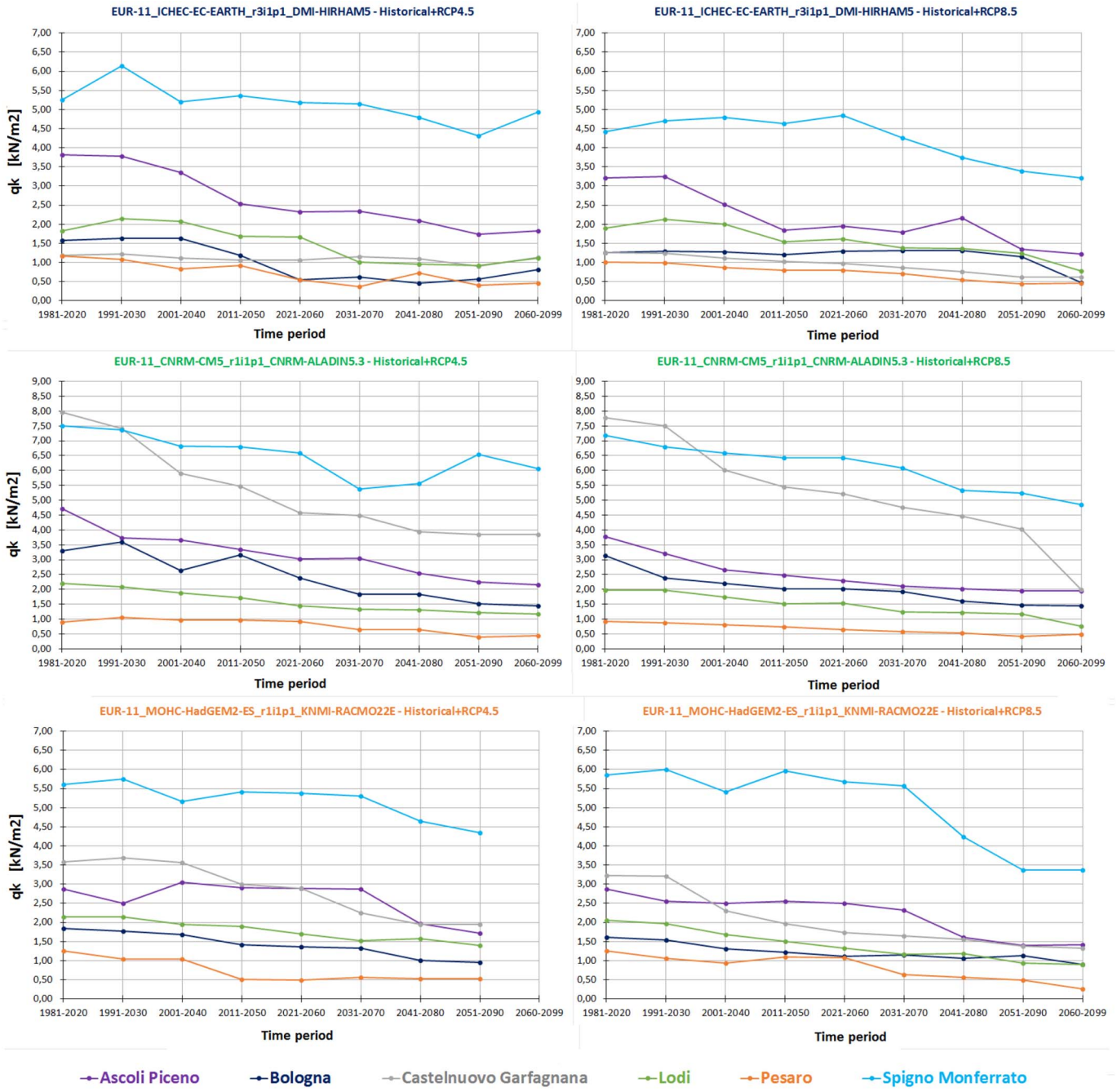

Fig. 11. Predicted variations over time of q_k [kN/m^2] till 2100 for different climate models and scenarios.

shifted by 10 years.

Finally, to assess the variability of climate models and scenarios, for the nine investigated stations the characteristic values of ground snow loads associated to different scenarios ($q_{kRCP4.5}$ and $q_{kRCP8.5}$) and to each time window in the period 1981–2100 have been compared, adopting different climate models. The outcomes of the comparison, in terms of ratio between $q_{kRCP8.5}$ and $q_{kRCP4.5}$, are diagrammatically shown in Fig. 12.

The results show a general decrease of characteristic ground snow loads at the investigated stations, but the expected decreasing trend of the ratio $q_{kRCP8.5}/q_{kRCP4.5}$, namely a more significant decrease of snow loads linked to increasing emissions, is not confirmed for all of them.

Extending the analysis illustrated above to a larger number of weather stations it is possible to obtain enough local information to update snow maps. The updated versions of the maps, critically compared with the current versions (EN 1991-1-3, 2004), will provide a comprehensive overview of the impact of climate change, according to different RCP scenarios.

5. Preliminary results on snow map comparison

The proposed procedure seems very appropriate for creation of snow maps taking into account the effects of climate change, since it allows to estimate characteristic ground snow loads on the basis of daily data for the minimum and maximum temperature and precipitation, which are typically available outputs of climate change projections for each relevant RCP scenario.

However, to derive consistent snow maps, further calibration is needed.

Indeed, climate projections are provided, in the higher resolution

Fig. 12. Time variation of the ratio between $q_{kRCP8.5}$ and $q_{kRCP4.5}$ for different climate models and different stations.

models, for geographical square cells of about 12,5 × 12,5 km (EUR11 - 0,11° on a rotated grid) and are generally agreed to represent area averaged data rather than point process data, especially for precipitation data (Haylock et al., 2008). Therefore, the analysis of gridded data can lead to an underestimation of extremes (Haylock et al., 2008) (Mannashardt-Shamseldin et al., 2010) and of micro-climate effects, depending on the local orography.

5.1. Comparison of observed gridded data and observed point data

In order to assess a calibration method for the analysis of gridded datasets, able to take into account the expected underestimation of extremes and the effects of local orography, the above mentioned issue has been especially studied for Italy, comparing the characteristic ground snow loads obtained by:

- the European Snow Load Research Project (ESLRP) for the weather stations in Mediterranean region (DGII-D3, 1998), which are reported on the grid cell map of E-OBS in Fig. 13;
- the analysis of observed grid cell data provided by the European Climate Assessment & Dataset project (E-OBS dataset (Haylock et al., 2008)) for the period 1951–1990, according to the procedure illustrated in the previous paragraph and assuming, consistently with the conclusions of the discussion summarized in Section 4.3, a constant correction factor, k_{corr}, for each of the four climatic zones defined by EN1991-1-3 for the Mediterranean region covering Italy. In this case, the correction factor for a given zone has been set equal to the mean value for the zone, according to Table 4.

The characteristic snow loads for the above mentioned four climatic zones are plotted as a function of the site altitude in Figs. 14, 15, 16 and 17, respectively; they confirm that, except for Zone 1, characteristic values computed by the analysis of gridded data (q_{kEOBS}) are typically lower than values obtained by point-data (q_{kESLRP}) and that the difference

$$\Delta q_k = q_{kESLRP} - q_{kEOBS} \tag{13}$$

generally increases with the altitude of the site.

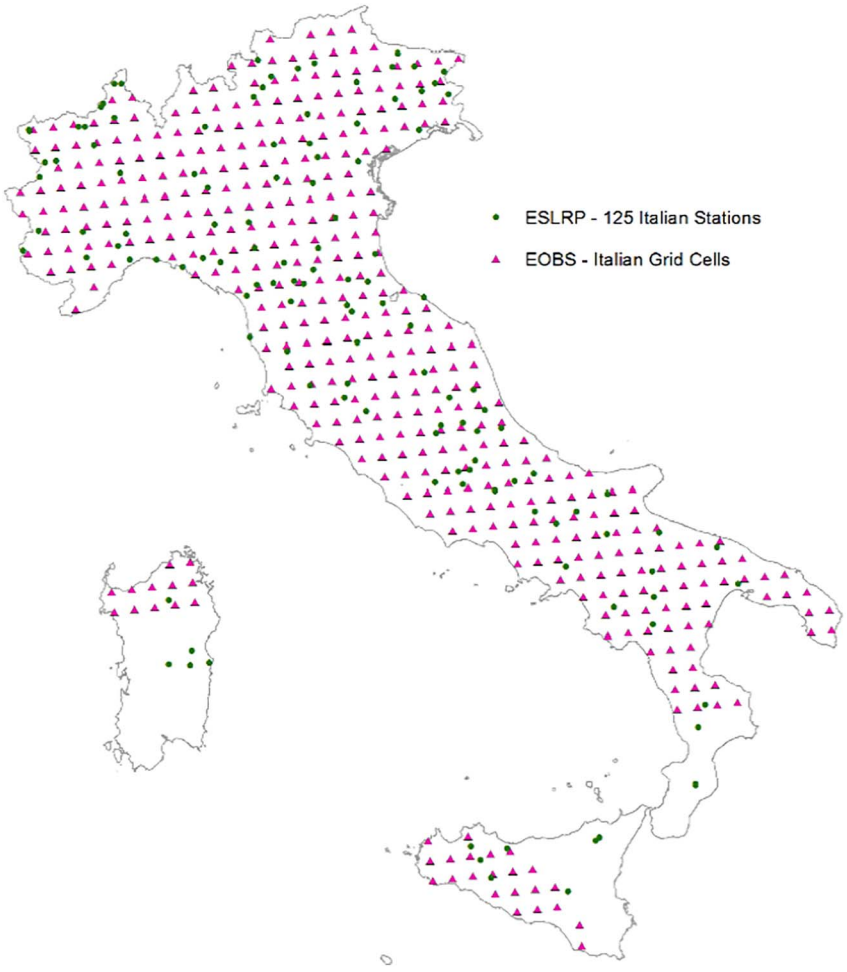

Fig. 13. E-OBS – Grid Cells and ESLRP weather stations for Italy.

Table 4
Correction factor for the climatic zones defined by EN1991-1-3 for the Mediterranean region in Italy.

ZONE - EN1991-1-3	$K_{corr} = q_k/q_{KESLRP}$
1	2,63
2	1,42
3	1,96
4	1,69

Subsequently, starting from these results, a calibration procedure has been defined in two steps:

- first, a regression analysis has been carried out in order to derive an altitude relationship for q_{kEOBS} data in each climatic zone (purple lines in Figs. 14–17)

$$q'_{kEOBS}(A) = \left[a + \left(\frac{A}{b}\right)^2\right]\frac{kN}{m^2} \tag{14}$$

where A is the altitude of the site in [m] and a and b are two

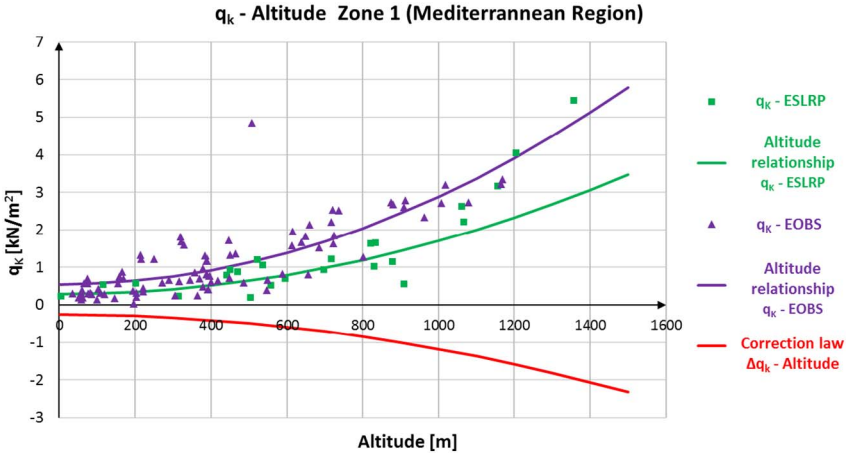

Fig. 14. q_k – Altitude curves (Italy - Mediterranean region - Zone 1).

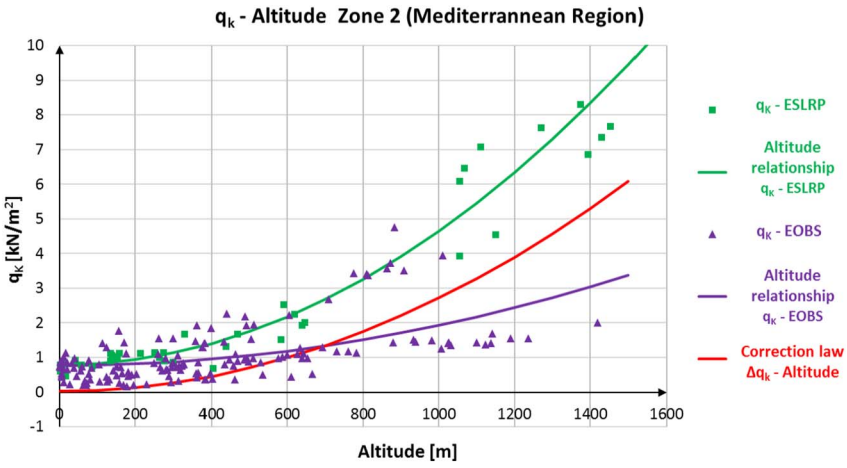

Fig. 15. q_k – Altitude curves (Italy Mediterranean region - Zone 2).

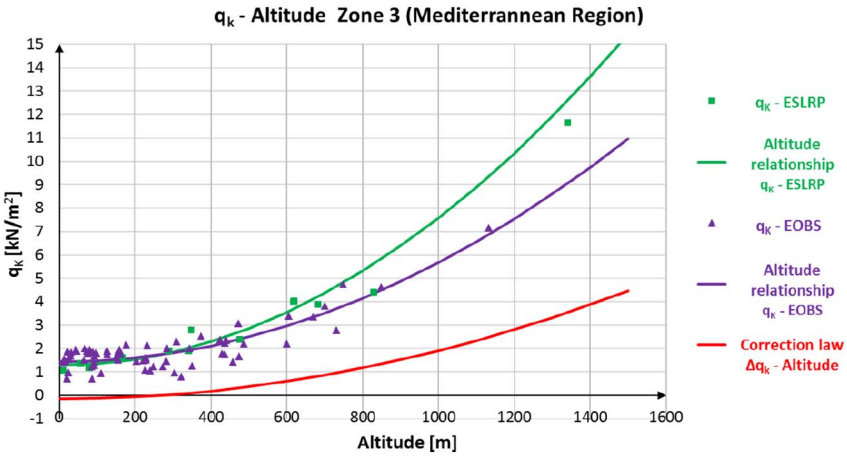

Fig. 16. q_k – Altitude curves (Italy Mediterranean region - Zone 3).

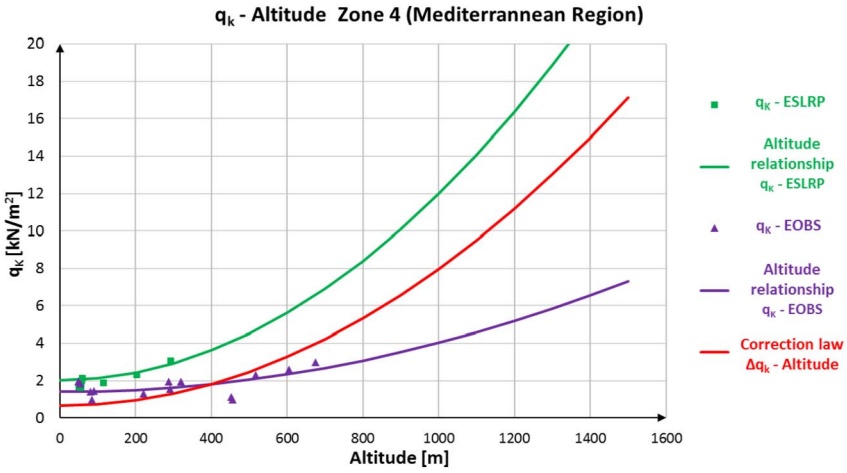

Fig. 17. q_k – Altitude curves (Italy Mediterranean region - Zone 4).

dimensionless coefficients determined via regression analysis;

- second, a correction rule has been defined for each climatic zone as

$$q_{k\mathrm{EOBS\ (corrected)}} = q'_{k\mathrm{EOBS}}(A) + \Delta q_k(A) \tag{15}$$

where the functions $\Delta q_k(A)$ (red lines in Figs. 14–17) are calculated as the difference between the altitude function for $q_{k\mathrm{ESLRP}}$ data, defined in (DGII-D3, 1998), and the altitude function $q_{k\mathrm{EOBS}}'(A)$ defined by Eq. (14).

Once these relationships are available, it is possible to draw, according to the results obtained by the analysis of gridded data, the snow load map on the ground consistent with the current version of snow map present in (EN 1991-1-3, 2004). The results are presented in Fig. 18 (before calibration) and Fig. 19 (after calibration).

The definition of the correction term $\Delta q_k(A)$ is very important because it allows to take into account also results obtained for characteristic ground snow loads by the investigation of projected data with respect to the current code's previsions.

Then, the next step will be the analysis of projected data, provided by different climate models, in order to derive maps of future variations of characteristic ground snow loads.

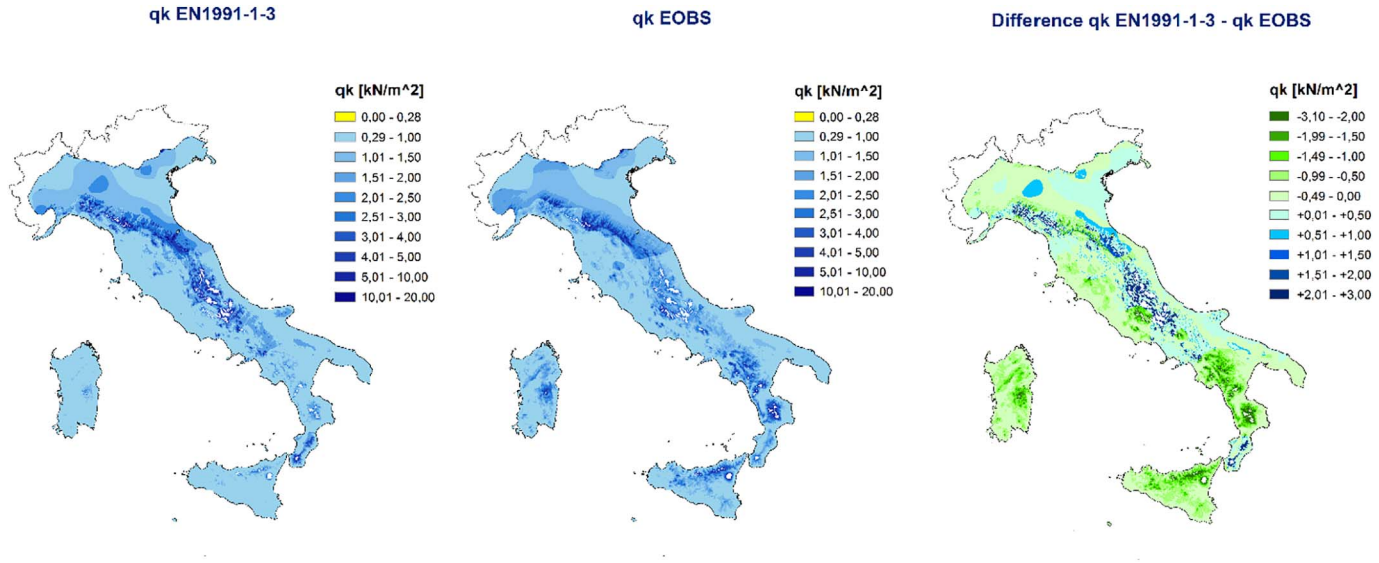

Fig. 18. Comparison of snow load map of EN1991-1-3 and snow load map obtained using EOBS data (before calibration).

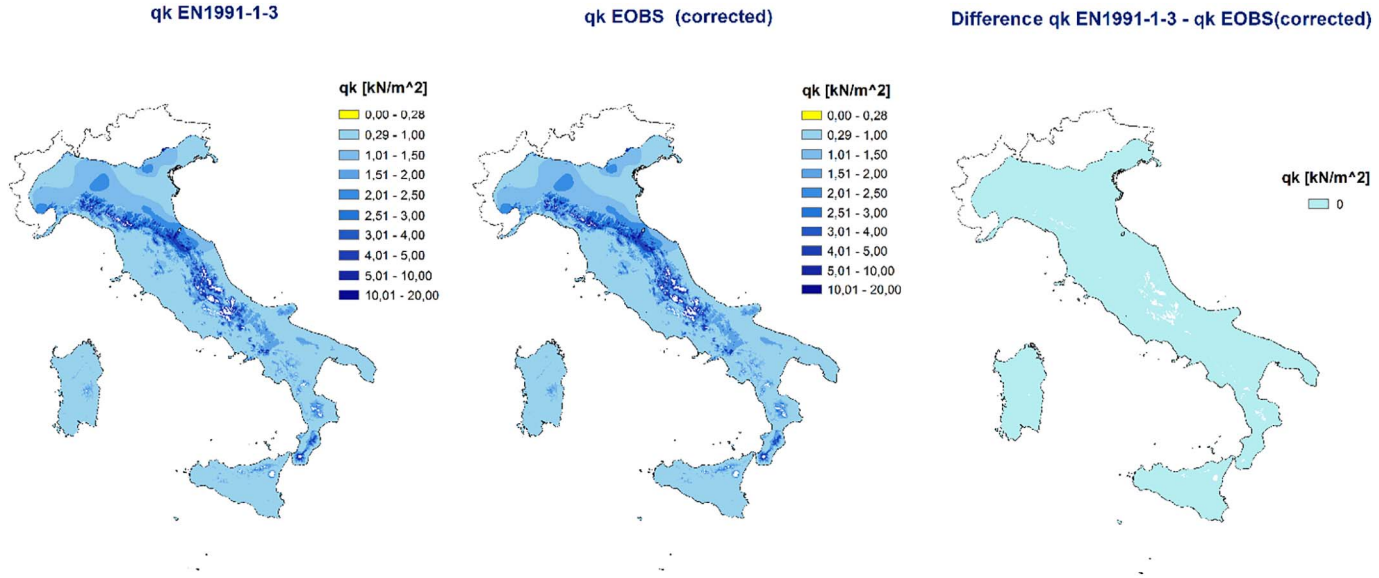

Fig. 19. Comparison of snow load map of EN1991-1-3 and snow load map obtained using EOBS data (after calibration).

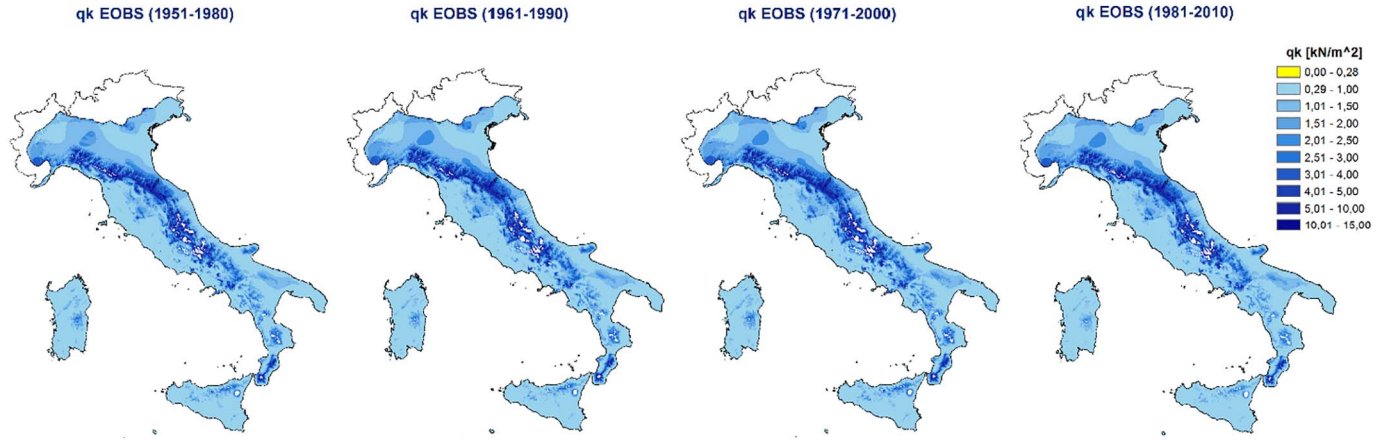

Fig. 20. Snow load maps obtained for different periods of EOBS data.

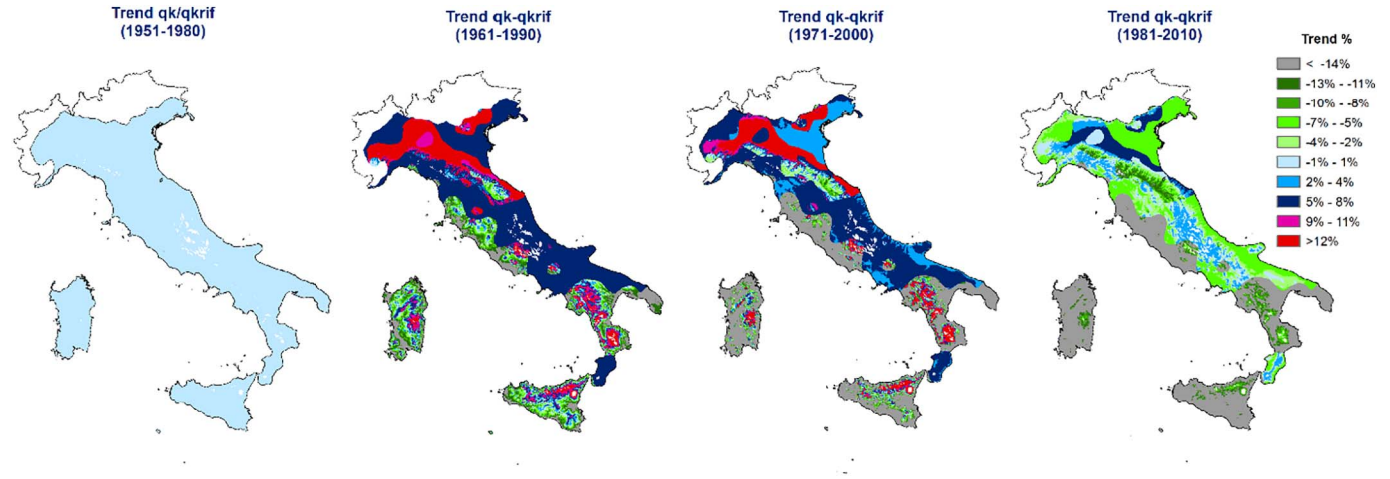

Fig. 21. Comparison of snow load maps with reference to the period 1951–1980.

5.2. Actual trend of variation of ground snow load

Before the study of projected data, which is currently in progress, EOBS gridded data for the Italian region have been analysed for subsequent time periods of thirty years, in order to estimate both the present trend of variation of characteristic ground snow loads and its future evolution.

The results are illustrated in Figs. 20 and 21 and show different trends for the Italian climatic zones. In fact, while in the northern and eastern Regions snow load is generally increasing, in western and southern Regions, except part of Tuscany and Campania, it tends to decrease.

6. Conclusions

Implications of climate change on snow loads could have very high impact on design of structures as well as on assessment of existing ones. The problem is very relevant as it is demonstrated by a high number of structural collapses of lightweight structures due to snow.

For this reason, the setup of a suitable procedure to predict the snow load on ground according to various climate change scenarios could represents a very strong improvement in definition and adaption of snow load maps. This issue is particularly relevant in Europe, especially in view of the development of future generation of Eurocodes.

Aiming to tackle this relevant issue, a general procedure to evaluate future trends of ground snow loads for structural design, taking into account the influence of climate change is proposed, based on Monte Carlo method.

The procedure, starting from the analysis of historical meteorological observations, allows to estimate ground snow loads and their characteristic values, on the basis of daily outputs of climate models, which are typically available as daily air temperature extremes (T_{max} and T_{min}) and height of precipitation (h_r).

The preliminary implementation of the outlined procedure is very promising and shows that there is a concrete possibility to arrive to define a general methodology for the estimate of characteristic ground snow loads, according to predictions derived from climatological models, also at a local scale. Since the presented methodology seems to be able to appreciate the evolution of the snow load during the time, it should also allow proper refinement and updating of the snow load maps according the real trends, or even adaption of them in terms of real evolution of climate change.

By extending the analysis to predicted data series covering a sufficiently large number of weather stations across Europe, it will be possible to draw snow maps for each available greenhouse gas emission scenario, to be compared with the existing ones. In this way, according to the requests of the European Commission to CEN (M/515 EN, 2012) within the European policy for the adaptation to climate change and in view of the development of the second generation of Eurocodes, it should be possible to assess how the climate change governs the evolution of ground snow loads and how much it is likely to influence structural reliability of new structures as well as of the built environment.

Acknowledgement

We acknowledge the World Climate Research Programme's Working Group on Regional Climate, and the Working Group on Coupled Modelling, former coordinating body of CORDEX and responsible panel for CMIP5. We also thank the climate modelling groups (listed in Table 2 of this paper) for producing and making available their model output. We also acknowledge the Earth System Grid Federation infrastructure an international effort led by the U.S. Department of Energy's Program for Climate Model Diagnosis and Intercomparison, the European Network for Earth System Modelling and other partners in the Global Organisation for Earth System Science Portals (GO-ESSP).

References

Biegus, A., Rykaluk, K., 2009. Collapse of Katowice Fair Building. Eng. Fail. Anal. 16, 1643–1654.
CAN/CSA - S502-14, 2014. Managing Changing Snow Load Risk for Building in Canada's North, CSA Group, Toronto.
CEN/TC250, 2013. Response to Mandate M/515 - Towards a Second Generation of Eurocodes, CEN-TC250 - N 993.
DGII-D3, 1998. Scientific Support Activity in the Field of Structural Stability of Civil Engineering Works. Snow Loads - FINAL REPORT.
EN 1991-1-3, 2004. Eurocode 1: Actions on Structures – Part 1–3: General Actions – Snow Loads, CEN, Brussels.
European Commission, 2013a. An EU Strategy on Adaptation to Climate Change, COM 213 Final Report.
European Commission, 2013b. Adapting Infrastructure to Climate Change, SWD 137 Final Report.
European Environment Agency, 2012. Climate Change, Impacts and Vulnerability in Europe, EEA Report n°12.
Früwald, E., Serrano, E., Toratti, T., et al., 2007. "Design of Safe Timber Structures - How Can We Learn from Structural Failures in Concrete, Steel and Timber?", Report TVBK-3053. Lund University, Lund.
Geis, J., Strobel, K., Liel, A., 2012. Snow induced building failures. J. Perform. Constr. Facil. 26 (4), 377–388.
Goodison, B.E., Louie, P.Y.T., Yang, D., 1998. WMO - Solid Precipitation Measurement Intercomparison – Final Report, WMO/TD N872.
Haylock, M.R., Hosfra, N., Klein Tank, A.M.G., et al., 2008. A European daily high-resolution gridded data set of surface temperature and precipitation for 1950–2006. J. Geophys. Res. 113.
Holicky, M., 2007. Safety design of lightweight roofs exposed to snow load. Eng. Sci. 58, 51–57.
Holicky, M., Sykora, M., 2009. Failures of roofs under snow load: causes and reliability analysis. Forensic Engineering 444–453.

Jacob, D., Petersen, J., Eggert, B., et al., 2014. EURO-CORDEX: new high-resolution climate change projections for European impact research. Reg. Environ. Chang. 14, 563–578.
Kotlarsky, S., Keuler, K., Christensen, O.B., et al., 2014. Regional climate modelling on European scale: a joint standard evaluation of the EURO-CORDEX ensemble. Geosci. Model Dev. 7, 1297–1333.
Lendvai, A., Ranzi, R., Peretti, G., et al., 2014. Misura delle precipitazioni nevose mediante i pluviometri. AINEVA- Neve e Valanghe 84, 12–21.
M/515 EN, 2012. Mandate for Amending Existing Eurocodes and Extending the Scope of Structural Eurocodes, Brussels.
Mannashardt-Shamseldin, E.C., Smith, R.L., Sain, S.R., et al., 2010. Downscaling extremes: a comparison of extreme value distributions in point source and gridded precipitation data. Ann. Appl. Stat. 4, 484–502.
Mellor, M., 1965. Blowing Snow, Cold Regions Science and Egineering Part III, Section A3c.
Rasmussen, R., et al., 2012. How well we are measuring snow? Bull. Am. Meteorol. Soc. 93, 811–829.
Sevruk, B., 1983. Correction of measured precipitation in the Alps using the water equivalent of new snow. Nord. Hydrol. 15, 49–68.
Sevruk, B., 1986. Conversion of Snowfall Depths to Water Equivalents in the Swiss Alps. Zürcher Geographische Schriften, ETH Zürich 23, 13–23.
Strasser, U., 2008. Snow loads in a changing climate: new risks? Nat. Hazards Earth Syst. Sci. 8, 1–8.
Tayet, H.T.T., Hygen, H.O., Kvande, T., 2013. “Present and Future of Snow Loads in Norway”, EMS 2013-230 13th EMS/11th ECAM, Reading.
Taylor, K.E., Stouffer, R.J., Meehl, G.A., April 2012. An overview of CMIP5 and the experiment design. Bull. Am. Meteorol. Soc. 485–498.
U.S. Department of Commerce National Oceanic and Atmospheric Administration, 2013. Snow Measurement Guidelines for National Weather Service Surface Observing Programs.
Van Vuuren, D.P., Edmonds, J., Kainuma, M., et al., 2011. The representative concentration pathways: an overview. Clim. Chang. 109, 5–31.
WG1AR5-IPCC, 2013. Climate change. The physical Science Basis.
Yang, D., et al., 1998. Accuracy of NWS 80 standard nonrecording precipitation gauge: results and application of WMO intercomparison. J. Atmos. Ocean. Technol. 15, 54–68.